Applied Soft Computing 46 (2016) 588–595

Contents lists available at ScienceDirect

Applied Soft Computing

journal homepage: www.elsevier.com/locate/asoc

Multimodal medical image fusion using PCNN optimized by the QPSO algorithm

Xinzheng Xu [a,b,*], Dong Shan [a], Guanying Wang [a], Xiangying Jiang [a]

[a] School of Computer Science and Technology, China University of Mining and Technology, Xuzhou 221116, China
[b] Jiangsu Key Laboratory of Mine Mechanical and Electrical Equipment, China University of Mining and Technology, Xuzhou 221116, China

ARTICLE INFO

Article history:
Received 28 May 2015
Received in revised form 15 October 2015
Accepted 28 March 2016
Available online 7 May 2016

Keywords:
Multimodal medical image fusion
Pulse-coupled neural networks
Quantum-behaved particle swarm optimization algorithm
Mutual information

ABSTRACT

This paper proposed a method to fuse multimodal medical images using the adaptive pulse-coupled neural networks (PCNN), which was optimized by the quantum-behaved particle swarm optimization (QPSO) algorithm. In this fusion model, two source images, A and B, were first processed by the QPSO-PCNN model, respectively. Through the QPSO algorithm, the PCNN model could find the optimal parameters for the source images, A and B. To improve the efficiency and quality of QPSO, three evaluation criteria, image entropy (EN), average gradient (AG) and spatial frequency (SF) were selected as the hybrid fitness function. Then, the output of the fusion model was obtained by the judgment factor according to the firing maps of two source images, which maybe was the pixel value of the image A, or that of the image B, or the tradeoff value of them. Based on the output of the fusion model, the fused image was gained. Finally, we used five pairs of multimodal medical images as experimental data to test and verify the proposed method. Furthermore, the mutual information (MI), structural similarity (SSIM), image entropy (EN), etc. were used to judge the performances of different methods. The experimental results illustrated that the proposed method exhibited better performances.

1. Introduction

Image fusion is the process of collaboratively combining different sources of sensory information into one representational format [1,2], so that the fused images are suitable for human visual perception and computer processing. Medical image fusion has emerged as a hotspot issue due to the increasing demands of clinical applications [3]. It not only provides easy access to extract more useful information for diagnosing diseases but also reduces the storage cost by fusing the information of multiple images into a single image. In previous work, researchers have proposed numerous methods for medical image fusion, such as contrast pyramid [4], ratio pyramid, morphological pyramid, and Laplacian pyramid. However, these fusion methods have a common limit: each approach is suitable for one specific type of image and is not robust to others. Moreover, each method has its own shortcomings. For instance, the morphological pyramid method is likely to generate bad edges [5], and the images fused by contrast pyramid often lose too much information. Overall, the methods mentioned above cannot deal with various types of medical images.

PCNN was proposed by Eckhorn et al. [6] based on research on the synchronous pulse burst in the visual cortex of cats and monkeys. Therefore, PCNN has an important biological background, which makes it more capable for image processing such as image segmentation, image enhancement, and pattern recognition. Many researchers have focused on the theory and application of image fusion using PCNN. For example, Wang and Ma [7] proposed the m-PCNN model for medical image fusion. A remarkable characteristic of m-PCNN is that the number of external channels can easily be changed according to actual requirements, and this is very useful when several images are fused at the same time. Das and Sudeb [8] used PCNN and a modified spatial frequency to address multimodal medical image fusion. The main advantage of this method is that it uses the shift-invariance, multi-scale and multi-directional properties of NSCT along with the modified spatial frequency to motivate PCNN. In this manner, the images can be fused with high contrast, clarity and information. However, the above methods suffer from various problems, and one common problem is that the parameters of the PCNN model are difficult to set. The performance of the available method of image fusion using PCNN mentioned above is limited because PCNN has several parameters and all of them play important roles in the model. In addition, the appropriate values of

* Corresponding author at: School of Computer Science and Technology, China University of Mining and Technology, Xuzhou 221116, China.
E-mail addresses: xxzheng@cumt.edu.cn, xuxinzh@163.com (X. Xu).

http://dx.doi.org/10.1016/j.asoc.2016.03.028
1568-4946/

the parameters of the traditional PCNN model can only be adjusted manually or estimated through a large amount of training, which is not convenient or economical for a real system. Thus, this shortcoming hampers the performance of the PCNN model in the medical image fusion field [9].

When PCNN is used, its parameters should be defined in advance. Furthermore, these parameters would be adjusted when input images change. So, the researchers have to try more times to find a set of suitable parameters according to different input images. The above process searching suitable parameters is similar to the optimization process of intelligent optimization algorithms. Inspired by the above relevance, some researchers introduced intelligent optimization algorithms to optimize the parameters of PCNN, and proposed several adaptive PCNN models, such as GA-PCNN [10], PSO-PCNN [11–13], QPSO-PCNN [14], MDE-PCNN [15], and FOA-PCNN [16]. However, the above methods had their own shortcomings and need to be solved. For example, the fitness function of these optimization algorithms should be modified to improve the search efficiency and generalization ability. To address the parameter issue of the PCNN model, based on our former work [14], we presented an adaptive PCNN model in which the parameters of PCNN were optimized by the QPSO algorithm. QPSO, as a branch of PSO, is proposed based on the quantum mechanics and trajectory analysis of PSO. QPSO shines due to its simplicity, ease of implementation, and fine search capability, and it has been shown to offer good performance in solving a wide range of continuous optimization problems [17,18]. According to these characteristics of QPSO, a modified PCNN model using the QPSO algorithm was proposed. In this manner, the adaptive PCNN can successfully solve the problem posed by the parameters of the traditional PCNN model, which makes medical image fusion more adaptable, efficient and accurate. It has been proven by experimental results that QPSO-PCNN performs well in the fusion of medical images.

The rest of the paper is organized as follows. In Section 2, basic theories, including the PCNN model and the QPSO algorithm, are introduced. Section 3 presents the research methods proposed in this paper, covering the image fusion model, the definition of QPSO's parameters and the medical image fusion algorithm using QPSO-PCNN. Section 4 gives the experimental results and contrasts with other approaches, and then the performance of the proposed method is discussed. Conclusions and future work are summarized in Section 5.

2. Theoretical backgrounds

2.1. PCNN model

The inspiration for PCNN comes from mammals, which is different from that for conventional artificial neural networks. The relationship between the image pixels and PCNN's neurons is one-to-one. The neuron model of the standard PCNN model is shown in Fig. 1. Each neuron of PCNN consists of three compartments: the receptive field, the modulation field and the pulse generator.

Its mathematical model is described by the following equations [19]:

$$F_{ij}(n) = e^{-\alpha_F} F_{ij}(n-1) + V_F \sum_{kl} M_{ijkl} Y_{kl}(n-1) + S_{ij} \tag{1}$$

$$L_{ij}(n) = e^{-\alpha_L} F_{ij}(n-1) + V_L \sum_{kl} W_{ijkl} Y_{kl}(n-1) \tag{2}$$

$$U_{ij}(n) = F_{ij}(n)(1 + \beta L_{ij}(n)) \tag{3}$$

$$Y_{ij}(n) = \begin{cases} 1, & if \quad U_{ij}(n) > \theta_{ij}(n-1) \\ 0, & others \end{cases} \tag{4}$$

$$\theta_{ij}(n) = e^{-\alpha_\theta} \theta_{ij}(n-1) + V_\theta Y_{ij}(n-1) \tag{5}$$

In the above corresponding equations, both F_{ij} and L_{ij} represent the input channels of the PCNN model, namely the feedback input and the linking input of the neuron in the (i, j) position. S_{ij} is the external stimulus, and it determines the time of the neurons ignition in one firing cycle. M_{ijkl} and W_{ijkl} represent the local connection matrix, which can adjust the influence of each neuron in the neighborhood of the center neuron. β is the linking coefficient, Y_{ij} is the output of the neurons from the previous iteration, and its values are 0 or 1. α_F, α_L and α_θ are the attenuation time constants of F_{ij}, L_{ij} and θ_{ij}, respectively, and V_F, V_L and V_θ are the corresponding inherent voltage potentials.

The parameters of PCNN are still required to adjust with feedback iterations, which is time consuming and inconvenient. Eckhorn et al. [20] simplified the link input field and the feedback input field and proposed a simplified PCNN model, which was later cited by many scholars and known as the most classic simplified PCNN model (shown in Fig. 2). Its mathematical model is described by Eqs. (6)–(10).

$$F_{ij}(n) = S_{ij} \tag{6}$$

$$L_{ij}(n) = \sum W_{ijkl} Y_{ij} \tag{7}$$

$$U_{ij}(n) = F_{ij}(1 + \beta L_{ij}(n)) \tag{8}$$

$$\theta_{ij}(n) = e^{-\alpha_\theta} \theta_{ij}(n-1) + V_\theta Y_{ij}(n-1) \tag{9}$$

$$Y_{ij}(n) = \begin{cases} 1, & U_{ij}(n) \geq \theta_{ij}(n) \\ 0, & U_{ij}(n) < \theta_{ij}(n) \end{cases} \tag{10}$$

This simplified model is mainly reflected in that the input neurons in the F-channel only consider the impact of the gray values of the external images' pixels and in that the input neurons in the L-channel consider the influence of the neurons' outputs within eight neighborhoods in the previous time, which not only reduces the complexity of the algorithm but also saves time.

When PCNN is used for image fusion, a two-dimensional image matrix $P \times Q$ can be interpreted as a network constituted by $P \times Q$ neurons, and the input stimulus S_{ij} is equal to the gray value of the (i, j) pixel. When there are pixels that have similar gray values in the internal connection matrix M and W neighborhood, the pulse output generated by the stimulation of one pixel will arouse stimulation of corresponding neurons in the neighborhood for which pixels have similar gray values and generate a pulse output sequence Y, and this output relies on the parameters of the network. Obviously, Y includes the region, edge and texture information of the image. In this manner, the binary image made by the output sequence Y is the fused image using PCNN. Thus, the PCNN's parameters influence the results of image fusion.

2.2. QPSO algorithm

The PSO algorithm, as a simulation of the social behavior of bird flocks, was proposed by Kennedy [21]. It can be easily implemented and is computationally inexpensive because its memory and CPU speed requirements are low. Inspired by quantum mechanics, Sun et al. [22] proposed a novel variant of PSO, called the quantum-behaved particle swarm optimization (QPSO) algorithm, which can be theoretically guaranteed to find the optimal solution in a search space. In the QPSO algorithm, the state of the particle is depicted by a wave function instead of the position and velocity as in the PSO

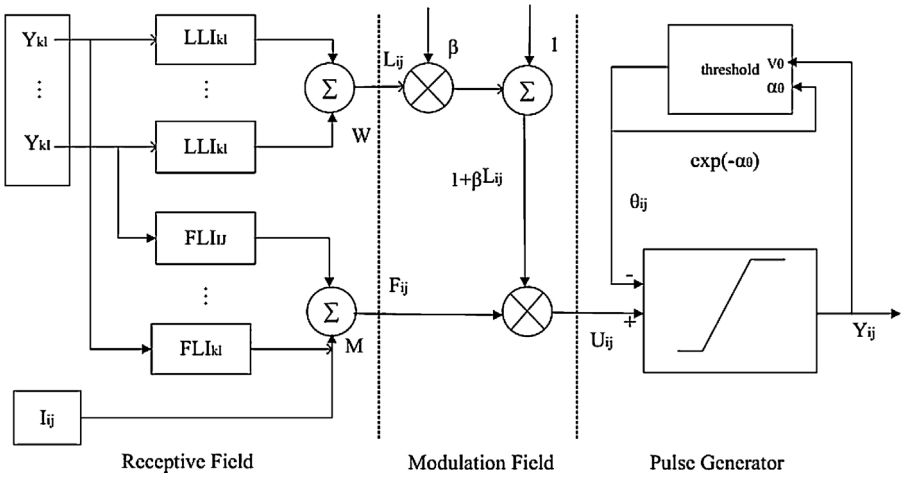

Fig. 1. Traditional model of a PCNN neuron.

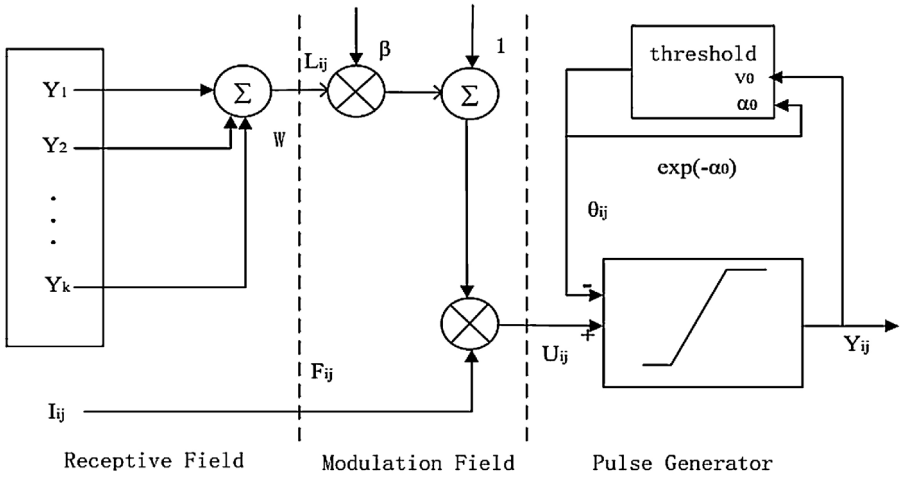

Fig. 2. Simplified model of a PCNN neuron.

algorithm. The dynamic behavior of the particle is widely divergent from that of the particle in classical PSO systems in that the exact values of position and velocity cannot be determined simultaneously.

In the tth iteration of the QPSO algorithm, the particles move according to the following iterative equation:

$$X_i(t+1) = PP_i(t) + \beta \mid Mbest_i(t+1) - X_i(t) \mid \times \ln(1/u) \quad if \quad k \geq 0.5$$
$$X_i(t+1) = PP_i(t) - \beta \mid Mbest_i(t+1) - X_i(t) \mid \times \ln(1/u) \quad if \quad k < 0.5 \tag{11}$$

where $X_i(t)$ is the position of the ith particle in the tth generation, u and k are random values distributed uniformly in the range [0,1], and β is a design parameter called the contraction-expansion coefficient, and can control the convergence speed of the particle. $PP_i(t)$ is the local attractor of the ith particle to guarantee convergence of the QPSO algorithm. $Mbest_i(t)$, called the mean best position, is defined as the mean of the best positions of all particles and is given by

$$Mbest_i(t) = \frac{1}{N}\sum_{j-1}^{N} P_j(t-1) \tag{12}$$

where N is the number of the particles in the swarm and $P_i(t-1)$ is the best position of the ith particle until the $(t-1)$th generation.

$PP_i(t)$ is calculated by the following equation:

$$PP_i(t) = P_i(t-1) + (1-\varphi)P_g(t-1) \tag{13}$$

where φ is a random value in the range [0,1] and $P_g(t-1)$ is the global best position of all particles until the $(t-1)$th generation.

At the end of each iteration, the best position of the ith particle $P_i(t)$ and the global best position of all particles $P_g(t)$ are updated after the fitnesses of all particles are calculated according to their new positions.

3. Research model developments

3.1. Definition of the fitness function and QPSO's parameters

3.1.1. Construction of the multi-criteria fitness function

In addition to evaluation by eye, the more objective evaluation method of image fusion is via multi-evaluation criteria. Thus, we should construct the fitness function according to the evaluation criterion. Moreover, the fitness function is also very important in influencing the performance of the QPSO algorithm. A good fitness function promotes particles to move from their initial position to the best position more quickly.

Considering these reasons, in this paper, we choose three commonly used evaluation criteria, image entropy (EN) [23], average gradient (AG) and spatial frequency (SF) [24], as the fitness function to effectually increase the search performance of the QPSO

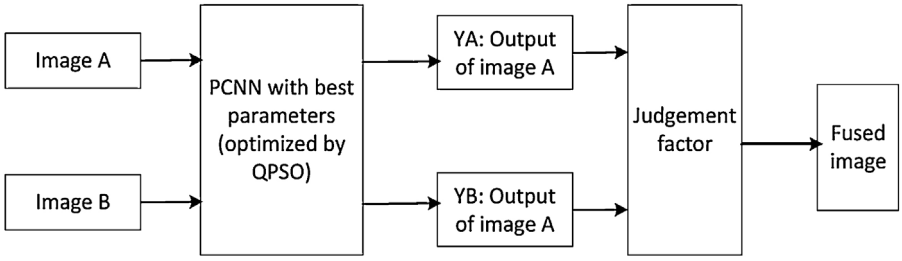

Fig. 3. Image fusion model based on QPSO-PCNN.

algorithm. Image entropy describes the amount of information an image contains, which means that, the larger the value of the entropy is, the more information the fused image contains. The average gradient is also called the image sharpness. It describes the details and texture feature of an image. Spatial frequency shows the degree of activity of the image space. The larger the value of SF is, the better the performance of the fusion method is. This paper adopts a multi-criteria fitness function shown as follows.

$$f = \max(SF + EN + AG) \tag{14}$$

3.1.2. Definition of other parameters

(1) Particle dimension: The dimensions of the particles represent the number of parameters to be solved. In the simplified PCNN model, there are 3 parameters (linking coefficient β, decay time constant α_θ, and threshold amplitude coefficient V_θ) to be determined, so the dimension of particles is 3 ($D = 3$).

(2) Population size: Population size has a strong influence on the robustness as well as on the complexity of the QPSO algorithm. Too small a population size may cause the problem of local convergence; however, too large a size may result in slow convergence and also increase the computational complexity. Usually, a population size ranging from 20 to 50 is appropriate. In this paper, the population size is 20 ($P = 20$).

(3) Terminal condition: The terminal condition of QPSO is generally to achieve the maximum iterative time or find the optimal fitness value to satisfy the threshold condition. In this work, the terminal condition of QPSO is limited by two aspects. One is that the algorithm cannot be executed for more than the maximal number of iterations, and the other is that the fitness values of ten consequent generations cannot exceed 0.01.

3.2. Image fusion method based on QPSO-PCNN

The model of image fusion based on QPSO-PCNN is shown in Fig. 3. Two source images, A and B, are first processed based on the QPSO-PCNN model, and then the most suitable parameters of the network are obtained, assuming that the scale of each neurons neighbors is $k * k$. Thus, two firing maps are generated, Y_A and Y_B, for the source images A and B, respectively. Next, the outputs are judged by the judgment factor. Therefore, we can determine whether the salient object exists in A or B based on the firing maps according to the situation of ignition time. The corresponding pixel value of pixel (i, j), namely $F(i, j)$, in the fused image is as follows.

$$F(i,j) = \begin{cases} [A(i,j) + B(i,j)]/2, & |Y_A(\bar{I},J) - Y_B(\bar{I},J)| < \varepsilon \\ A(i,j), & [|Y_A(\bar{I},J) - Y_B(\bar{I},J)| \geq \epsilon] \ \ and \ \ [Y_A(\bar{I},J) \geq Y_B(\bar{I},J)] \\ A(i,j), & [|Y_A(\bar{I},J) - Y_B(\bar{I},J)| \geq \epsilon] \ \ and \ \ [Y_A(\bar{I},J) \leq Y_B(\bar{I},J)] \end{cases} \tag{15}$$

where $Y_A(\bar{I}, J)$ and $Y_B(\bar{I}, J)$ are mean values for $Y_A(i, j)$ and $Y_B(i, j)$, i.e., the firing time of pixel (i, j) according to its neighbors' firing outputs. In this paper, the threshold adjustment constant $\Delta = 0.0705$, and the threshold value $\varepsilon = \Delta/2$.

The detailed procedures of the image fusion algorithm based on PCNN are shown in Algorithm 1.

Algorithm 1. Procedures of the image fusion algorithm based on PCNN

Require: parameters (β, α_θ, V_θ); // According to the QPSO-PCNN algorithm
Initialization;
[p, q] ← size (image);
For n=1: Times
  for i=1:p
    for j=1:q
      do: PCNN and calculate Y_A and Y_B; // According to Eqs. (6)–(10).
    end
  end
end
for i=1:p
  for j=1:q
    if $|Y_A(\bar{I}, J) - Y_B(\bar{I}, J)| < \epsilon$ F(i,j) ← [A(i,j) + B(i,j)]/2;
    else if $|Y_A(\bar{I}, J) - Y_B(\bar{I}, J)| \geq \epsilon$&&[$|Y_A(\bar{I}, J) > Y_B(\bar{I}, J)|$]F(i,j) ← A(i,j);
    else $|Y_A(\bar{I}, J) - Y_B(\bar{I}, J)| \geq \epsilon$&&[$|Y_A(\bar{I}, J) > Y_B(\bar{I}, J)|$]F(i,j) ← B(i,j);
    end if
  end
end
Return F

The procedures of the proposed QPSO-PCNN algorithm mainly include 6 steps, which are initialization, evaluation of the initial population, updating the positions of the particles, updating the best positions, checking the terminal condition and output of the best results. The detailed steps of the QPSO-PCNN algorithm are shown as Algorithm 2.

Algorithm 2. Procedures of the QPSO-PCNN algorithm:

Require: P=20, D=3, Times=100
For i=1: N
  Initialization (the value of each particle, local optimum and global optimum)
End
While (t<Times)
  For i=1: N
    $f_{current}(i) = SF + EN + AG$;
    If $pBest_{value} < f_{current}(i)$ $pBest_{value} = f_{current}(i)$;
    End if
    [iterbestval,idx1]=max($pBest_{value}$);
    if $gBest_{value} <$ iterbestval $gBest_{value} <$ iterbestval;
gbest=pbest(idx1,:);
    End if
    $MBest_i(t) = \frac{1}{N}\sum_{j=1}^{N} P_j(t-1)$
  End for
For d=1:D
  $PP_i(t) = P_i(t-1) + (1-\varphi)P_g(t-1)$
  $\begin{cases} X_i(\mathbf{t}) = PP_i(\mathbf{t}) + \beta|MBest_i(t) - X_i(t-1)| * \ln(1/u), \text{ , if k} \geq 0.5 \\ X_i(\mathbf{t}) = PP_i(\mathbf{t}) + \beta|MBest_i(t) - X_i(t-1)| * \ln(1/u), \text{ , if k} < 0.5 \end{cases}$
end
t = t + 1;
End while
[gBest_value, parameters]=max($gBest_{value}$);
Return parameters ($\boldsymbol{\beta}$, $\boldsymbol{\alpha_\theta}$, $\boldsymbol{V_\theta}$);

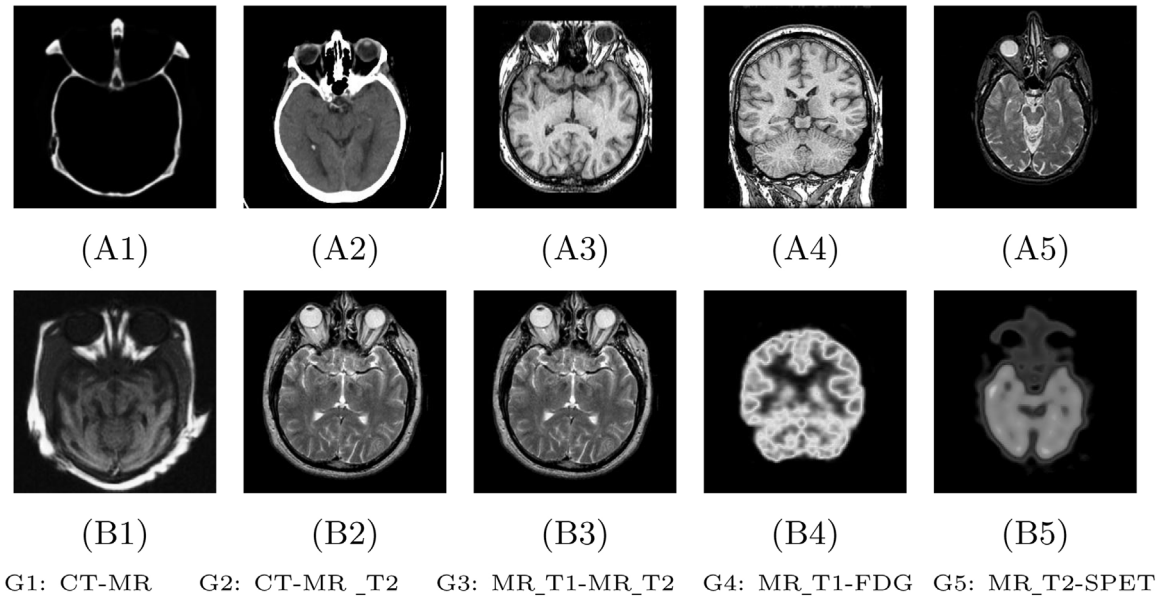

Fig. 4. Source images in different groups.

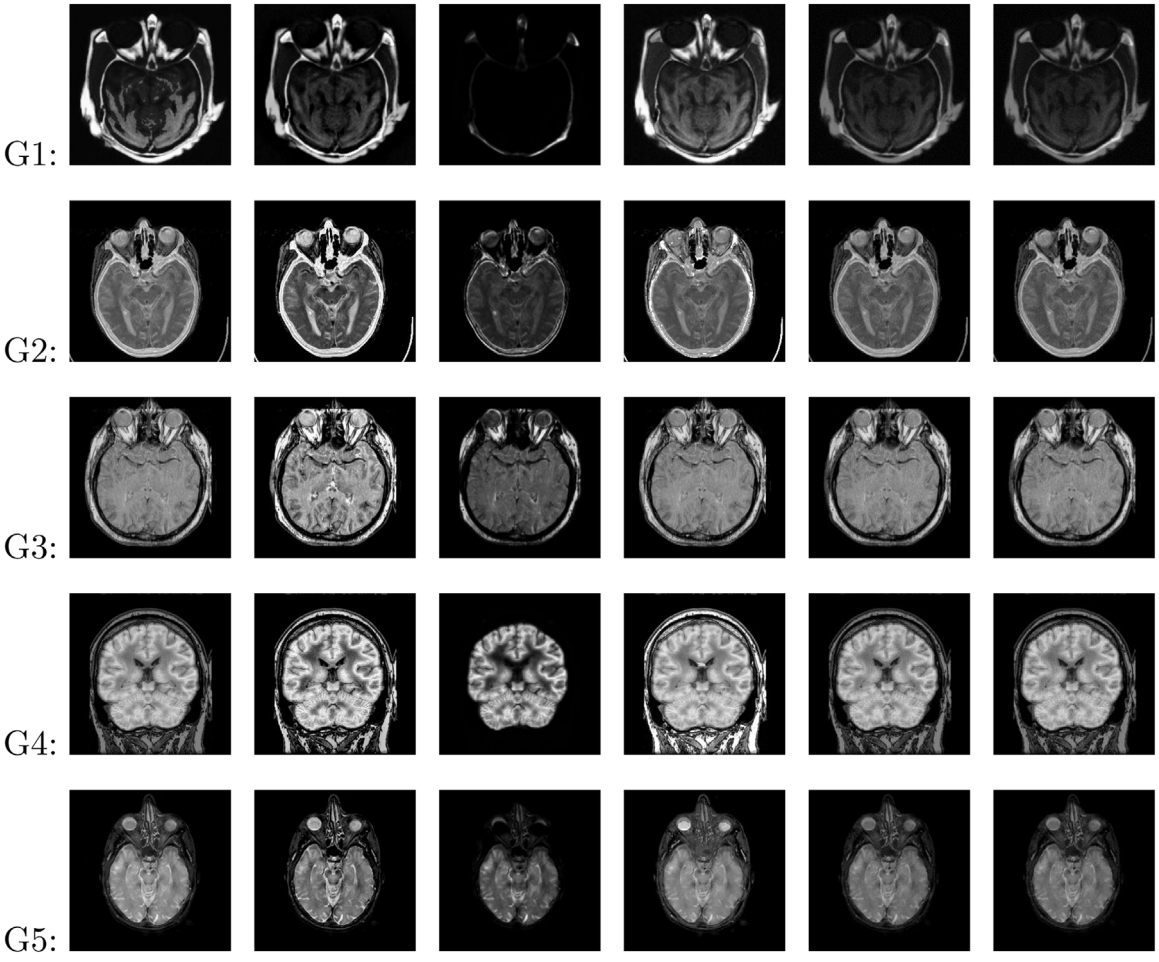

Fig. 5. Fusion results using different methods.

4. Experiment and analyses

In this work, experiments are conducted on five groups of 256-level images. Each group has two medical images of different types, which are shown in Fig. 4. Image A is one of the source images to be fused, and image B is another source image to be fused. The source images in group 1 (G1) can be download from the website (http://imagefusion.org), which is the Online Resource for research in image fusion. The source images of group 2 (G2) through group 5 (G5) are from the website of the Atlas project (http://www.med.harvard.edu/AANLIB), which is made possible in part by the Departments of Radiology and Neurology at Brigham and Womens Hospital, Harvard Medical School, the Countway Library of Medicine, and the American Academy of Neurology.

For the purpose of judging various methods objectively, in the first group experiments, image sharpness [25], mutual information (MI) [26], standard deviation (STD) [27], spatial frequency (SF) are used as the standard to estimate the performance of different methods. In groups 2–5, we used the structural similarity (SSIM) [28], image entropy and MI to estimate the performance of different methods. Image entropy describes the amount of information an image contains. The standard deviation represents the distribution of the image's pixel gray level. The higher the standard deviation is, the higher the contrast is. Wang et al. [28] proposed structural similarity (SSIM), which describes the similarity in structure of two images. Wang and Ma [29] used it as an objective evaluation index to evaluate the performance of the multi-focus image fusion. The MATLAB source code of SSIM can be downloaded from the website (http://www.cns.nyu.edu/~zwang/files/papers/ssim.html).

To show the performance of QPSO-PCNN, some other popular image fusion methods, such as Laplacian pyramid [30], and m-PCNN [7] with two channels (Dual-channel PCNN) are also used as comparison experiments. Besides, we compare our method with the existing hybrid methods such as MDE-PCNN [31] and EL-DC-PCNN [24]. Parameters of these methods are set as follows: the pyramid level is 4, and for selection rules, the high-pass equals select max and the low-pass equals average. The m-PCNN parameters are all taken from paper [7], and the parameters of the fusion method using the traditional PCNN with manual adjustment of the parameters are shown in Table 1 [23].

The source images are shown in Fig. 4. In group 1 (G1), A1 is a CT image and B1 is an MR image. In group 2 (G2), A2 is a CT image and B2 is an MR-T2 weighted image. In group 3 (G3), A3 is an MR-T1 weighted image, and B3 is an MR MR-T2 weighted image. In group 4 (G4), A4 is an MR-T1 weighted image, and B4 is an FDG image. In group 5 (G5), A5 is an MR-T2 weighted image, and B5 is an SPET image.

Table 1
Values of the traditional PCNN parameters, adjusted manually.

Parameters	α_F	α_L	α_θ	β	V_F	V_L	V_θ
Values	0.1	0.3	0.2	0.1	0.5	0.2	20

Table 2
Performances of different methods in group 1 (G1).

Methods	Sharpness	STD	SF	MI_AF	MI_BF	MI_AB
Our approach	7.6303	65.1832	22.8200	3.2100	0.5175	3.7275
Laplacian pyramid	7.0831	56.9984	19.6385	1.2386	0.3176	1.5562
Dual-channel PCNN	1.0256	15.3586	6.6391	0.4413	0.5297	0.9710
PCNN	6.9825	59.5184	18.2115	3.5335	0.4386	3.9721
MDE-PCNN	3.8764	34.8580	10.2662	3.1005	0.4543	3.5448
EL-DC-PCNN	3.8951	35.6541	9.9958	3.1210	0.4652	3.5862

Table 3
Performances of different methods in group 2 (G2) to group 5 (G5).

	Methods	Entropy	MI_AF	MI_BF	MI_AB	SSIM_AF	SSIM_BF
G2 (Group2): CT–MR_T2	Our approach	4.5362	1.7216	1.0066	2.7282	0.7667	0.6710
	Laplacian pyramid	4.5251	0.9577	0.9074	1.8651	0.7565	0.6626
	Dual-channel PCNN	3.9651	0.8961	0.8406	1.7367	0.6618	0.6710
	PCNN	4.4686	1.6942	0.9911	2.6853	0.7610	0.6498
	MDE-PCNN	4.5325	1.7190	1.0040	2.7230	0.7542	0.6745
	EL-DC-PCNN	4.5325	1.7202	1.0045	2.7247	0.7551	0.6706
G3 (Group3): MR_T1–MR_T2	Our approach	5.4726	2.1188	1.0928	3.2116	0.7954	0.5638
	Laplacian pyramid	5.1822	1.0499	0.6882	1.7381	0.7871	0.5590
	Dual-channel PCNN	4.1593	0.8725	1.0357	1.9082	0.5146	0.8507
	PCNN	5.2439	1.2419	1.3719	2.6138	0.7465	0.6590
	MDE-PCNN	5.2850	1.2068	1.3813	2.5881	0.7497	0.6703
	EL-DC-PCNN	5.3562	1.8953	1.0354	2.9307	0.7952	0.5621
G4 (Group4): MR_T1–FDG	Our approach	5.4726	2.1188	1.0928	3.2116	0.7954	0.5638
	Laplacian pyramid	5.1822	1.0499	0.6882	1.7381	0.7871	0.5590
	Dual-channel PCNN	4.1593	0.8725	1.0357	1.9082	0.5146	0.8507
	PCNN	5.3688	2.1402	0.9973	3.1375	0.8588	0.5620
	MDE-PCNN	5.4192	2.0866	1.0557	3.1432	0.7674	0.5665
	EL-DC-PCNN	5.4295	2.1100	1.0655	3.1500	0.7765	0.5622
G5 (Group5): MR_T2–SPET	Our approach	3.7875	1.3129	1.1263	2.4392	0.8751	0.7368
	Laplacian pyramid	3.5613	0.9958	0.6532	1.6490	0.9388	0.6612
	Dual-channel PCNN	3.1897	0.8435	0.8541	1.6976	0.7464	0.7637
	PCNN	3.7717	1.2746	1.1194	2.3940	0.8522	0.7466
	MDE-PCNN	3.7204	1.2768	1.0463	2.3231	0.8765	0.7375
	EL-DC-PCNN	3.6920	1.2770	1.1002	2.3772	0.8720	0.7352

The fusion results using different methods are shown in Fig. 5. Gi means group i. The first column images are fused by our method. The second, third, fourth and fifth column images are fused by the Laplacian pyramid method, m-PCNN with two channels (Dual-channel PCNN), traditional PCNN with the parameters adjusted manually, MDE-PCNN and EL-DC-PCNN, respectively.

The source images of MR and CT images are commonly used to test the performances of different fusion methods, so in group 1, we used mutual information (MI), standard deviation (STD), image sharpness, and spatial frequency (SF) as the evaluation standard for the performances of different methods. The values are shown in Table 2, and the fused images are shown in the first row of Fig. 5.

In Tables 2 and 3, MI_AF and MI_BF represent the MI between the source image A and the fused image and the MI between the source image B and the fused image, respectively [7]. The MI_AB refers to the sum of MI_AF and MI_AF, which shows the abilities of the fused images to acquire information from two source images.

From Table 2, we can see that the values of image sharpness, STD and SF by our method are far larger than the values by the other three methods, which shows that our method can achieve better results.

In group 2 (G2) to group 5 (G5), we experiment on CT–MR_T2 images, MR_T1–MR_T2 images, MR_T1–FDG images and MR_T2–SPET images. The image entropy (EN), structural similarity (SSIM), and mutual information (MI) are used to evaluate the performance of different methods. The fused results by different methods are shown in Fig. 5, and the performances of each method in group 2 to group 5 are presented in Table 3. SSIM_AF represents the structural similarity between the source image A and the fused image, while SSIM_BF represents the structural similarity between the source image B and the fused image.

Because the dual-channel PCNN model is essentially a neuron network without feedback, the performance of the dual-channel PCNN depends on the value of the initial threshold. As seen from Fig. 5, the images fused by dual-channel PCNN lose too much information. However, the images fused by our method obtain the best results. The order of other methods changes with different source images, but our method always performs best, which shows that the other methods have poor flexibility and stability while our method has strong robustness to different source images. From the quantitative analysis, it can be seen that the images fused by our approach not only contain the richest information from source images but also have better structure similarity with the source images.

From the above analysis and discussion, a conclusion can be drawn that the proposed approach outperforms other image fusion methods for medical images. Our method can not only adjust to different types of medical images but also acquire more information from source images, which is useful for doctors and their diagnoses. However, it also can be found that images fused by our approach are not as good as some other methods in image sharpness except in group 1, which is also a problem we will solve in subsequent research.

5. Conclusions

Medical image fusion plays an increasingly significant role in clinical applications. PCNN is a suitable and efficient approach for medical image fusion. However, all medical image fusion methods based on PCNN have a common problem in that the parameters are hard to set, which renders the methods less practical and accurate. We have proposed QPSO-PCNN to solve such problems. In this paper, five pairs of medical images are used to test the performance of the QPSO-PCNN medical image fusion method against other methods, and the results prove that our method is superior to the other methods. Its efficiency, convenience and accuracy demonstrate that our method is very suitable for medical image fusion.

Acknowledgements

This work is supported by the Fundamental Research Funds for the Central Universities (No. 2015XKMS088).

References

[1] C.P. Behrenbruch, K. Marias, P.A. Armitage, et al., Fusion of contrast-enhanced breast MR and mammographic imaging data, Med. Image Anal. 7 (3) (2003) 311–340.
[2] Z.B. Wang, Y.D. Ma, Dual-channel PCNN and its application in the field of image fusion, in: International Conference on Natural Computation, Haikou, China, IEEE, Piscataway, USA, 2007, pp. 755–759.
[3] L. Wang, B. Li, L.F. Tian, A novel multi-modal medical image fusion method based on shift-invariant shearlet transform, Imaging Sci. J. 61 (7) (2013) 529–540.
[4] D.X. He, Y. Meng, C.Y. Wang, Contrast pyramid based image fusion scheme for infrared image and visible image, in: 2011 IEEE International conference on Geoscience and Remote Sensing Symposium (IGARSS), Vancouver, Canada, IEEE, Piscataway, USA, 2011, pp. 597–600.
[5] A. Toet, A morphological pyramidal image decomposition, Pattern Recognit. Lett. 9 (4) (1989) 255–261.
[6] R. Eckhorn, H.J. Reitboeck, M. Arndt, et al., A neural network for feature linking via synchronous activity: Results from cat visual cortex and from simulations, in: Models of Brain Function, Cambridge Univ. Press, London, 1989.
[7] Z.B. Wang, Y.D. Ma, Medical image fusion using m-PCNN, Inf. Fusion 9 (2) (2008) 176–185.
[8] S. Das, M.K. Kundu, NSCT-based multimodal medical image fusion using pulse-coupled neural network and modified spatial frequency, Med. Biol. Eng. Comput. 50 (10) (2012) 1105–1114.
[9] Y.M. Zhao, The PCNN adaptive segmentation algorithm based on visual perception, in: Third International Conference on Photonics and Image in Agriculture Engineering, Sanya, China, SPIE, Bellingham, USA, 2013.
[10] D. Zhang, S. Mabu, K. Hirasawa, Image denoising using pulse coupled neural network with an adaptive Pareto genetic algorithm, IEEJ Trans. Electr. Electron. Eng. 6 (5) (2011) 474–482.
[11] X.Z. Xu, S.F. Ding, Z.P. Zhao, H. Zhu, Particle swarm optimization for automatic parameters determination of pulse coupled neural network, J. Comput. 6 (8) (2011) 1546–1553.
[12] J. Wang, F. Cong, Grayscale image edge detection based on pulse-coupled neural network and particle swarm optimization, 2008 Chinese Control and Decision Conference (CCDC) (2008) 2576–2579.
[13] I.S. Hage, R.F. Hamade, Segmentation of histology slides of cortical bone using pulse coupled neural networks optimized by particle-swarm optimization, Comput. Med. Imaging Graphics 37 (7–8) (2013) 466–474.
[14] X.Z. Xu, S.F. Ding, Z.Z. Shi, H. Zhu, Z.P. Zhao, A self-adaptive method for optimization the parameters of pulse coupled neural network based QPSO algorithm, Pattern Recognit. Artif. Intell. 25 (6) (2012) 909–915.
[15] X.Y. Jiang, A self-adapting pulse-coupled neural network based on modified differential evolution algorithm and its application on image segmentation, Int. J. Digit. Content Technol. Appl. 6 (20) (2012) 501–509.
[16] H. Zhao, S.F. Ding, Study of automated PCNN system based on fruit fly optimization algorithm, J. Comput. Inf. Syst. 10 (15) (2014) 6635–6642.
[17] J. Sun, C.H. Lai, W. Xu, et al., A modified quantum-behaved particle swarm optimization, in: 7th International Conference on Computational Science, Beijing, China, Springer Verlag, Heidelberg, Germany, 2007, pp. 294–301.
[18] W. Fang, J. Sun, Y. Ding, et al., A review of quantum-behaved particle swarm optimization, IETE Tech. Rev. 27 (4) (2010) 336–347.
[19] Y.D. Ma, L. Li, Y.F. Wang, et al., Principle of Pulse-coupled Neural Network and its Applications, Science Press, Beijing, China, 2006, pp. 1–20.
[20] R. Eckhorn, H.J. Reitboeck, M. Arndt, Feature linking via synchronization among distributed assemblies: simulations of results from cat visual cortex, Neural Comput. 2 (3) (1990) 293–307.
[21] J. Kennedy, R. Eberhart, Particle swarm optimization, in: IEEE International Conference on Neural Networks, Perth, WA, IEEE, Piscataway, USA, 1995, pp. 1942–1948.
[22] J. Sun, B. Feng, W.B. Xu, Particle swarm optimization with particles having quantum behavior, in: Congress on Evolutionary Computation, Portland, USA, IEEE, Piscataway, USA, 2004, pp. 326–331.
[23] Y.D. Ma, R.L. Dai, L. Li, Automated image segmentation using pulse coupled neural networks and images entropy, J. China Inst. Commun. 23 (1) (2002) 46–51.
[24] Y. Li, X.J. Wu, A novel image fusion method using self-adaptive dual-channel pulse coupled neural networks based on PSO evolutionary learning, Acta Electron. Sinica 42 (2) (2014) 217–222.
[25] Y.D. Ma, K. Zhan, Z.B. Wang, Image Fusion Applications of Pulse-Coupled Neural Network, 2010, pp. 83–109.
[26] M. Seetha, I.V. MuraliKrishna, B.L. Deekshatulu, Data fusion performance analysis based on conventional and wavelet transform techniques, in: IEEE

Proceedings on Geoscience and Remote Sensing Symposium, vol. 4, 2005, pp. 2842–2845.
[27] Y. Zhao, Q. Zhao, A. Hao, Multimodal medical image fusion using improved multi-channel PCNN, Bio-medical Mater. Eng. 24 (1) (2014) 221–228.
[28] Z. Wang, A.C. Bovik, H.R. Sheikh, et al., Image quality assessment: from error visibility to structural similarity, IEEE Trans. Image Process. 13 (4) (2004) 600–612.
[29] Z.B. Wang, Y.D. Ma, J. Gu, Multi-focus image fusion using PCNN, Pattern Recognit. 43 (6) (2010) 2003–2016.
[30] P.J. Burt, E.H. Adelson, The Laplacian pyramid as a compact image code, IEEE Trans. Commun. COM-31 (4) (1983) 532–540.
[31] G.Y. Wang, X.Z. Xu, X.Y. Jiang, R. Nie, A modified model of pulse coupled neural networks with adaptive parameters and its application on image fusion, ICIC Express Lett. 6 (9) (2015) 2523–2530.